MOLECULAR SPIRAL STRUCTURE IN MESSIER 51 FROM ^{12}CO(2–1) AND (1–0) SINGLE-DISH OBSERVATIONS

S. GARCÍA-BURILLO[1,2] AND M. GUÉLIN[1]
[1] IRAM, 300 rue de la piscine, 38406 St-Martin-D'Heres, France
[2] Centro Astronómico de Yebes, Apdo.148 E-19080 Guadalajara, Spain

ABSTRACT. We present the first results of a high angular resolution–high sensitivity survey of CO (J=1–0) and (2–1) emission in M 51, made with the IRAM 30 m telescope. Of all tracers of the inner spiral structure, CO, i.e. presumably the molecular gas, appears as the tracer with the smoothest in-arm distribution, the highest arm-interarm contrast and the most visible streaming motions. Although observed about everywhere, CO, in the interarm region, is mostly concentrated along 4 radial lanes, or bridges, connecting the two main spiral arms.

We have mapped with full sampling (i.e. with a $6'' \times 6''$ spacing grid) the J= 2–1 and 1–0 line emission of ^{12}CO throughout the central $3.5' \times 3.5'$ area of M 51, using the IRAM 30 m telescope. The (2-1) and (1-0) lines of ^{13}CO were also observed at selected positions. The angular resolution was $12''$ (HPBW) in the (1-0) line and $21''$ in the (2-1) line. Special care was taken during the observing to insure a good pointing and a proper calibration. In particular, the error beam was measured by means of scans across the Moon and of long integrations on two interarm positions, located at $\pm$ 1 arc min. from the centre of M 51. Throughout this paper, intensities are expressed in the form of T_a^*, the equivalent antenna temperature reported above atmosphere.

M 51 was selected for this pilot investigation as the closest galaxy with a grand design spiral pattern and a strong CO emission, hence as the best object for studying the interplay of molecular clouds with spiral structure. At the distance of M 51 (9.6 Mpc), the $12''$ resolution in the (2–1) line of CO corresponds to 560 pc.

Figure 1 shows the ^{12}CO(2–1) velocity-integrated intensity contours. The two-arm spiral pattern stands out clearly and can be followed from the bright center of M 51, the central molecular disk, to the edges of the map, which, presumably, are close to the co-rotation region (see Tully, 1974). The CO arms are broad and, except $1'$ southwest of the centre where the arm is shifted outwards, follow closely the 20 cm non-thermal radio emission observed by van der Hulst et al. (1988). Within the area covered by Fig. 1, CO is detected about everywhere between the arms and exhibits bright structures, such as interarm bridges or spurs, superposed on a low intensity component.

Vogel et al. (1988) and Rand and Kulkarni (1990) have observed the area of Fig. 1 in the ^{12}CO(1–0) line, using the OVRO interferometer. Their $7'' \times 10''$ angular resolution

F. Combes and F. Casoli (eds.), Dynamics of Galaxies and Their Molecular Cloud Distributions, 67–71.
© 1991 *IAU. Printed in the Netherlands.*

https://doi.org/10.1017/S0074180900243556 Published online by Cambridge University Press

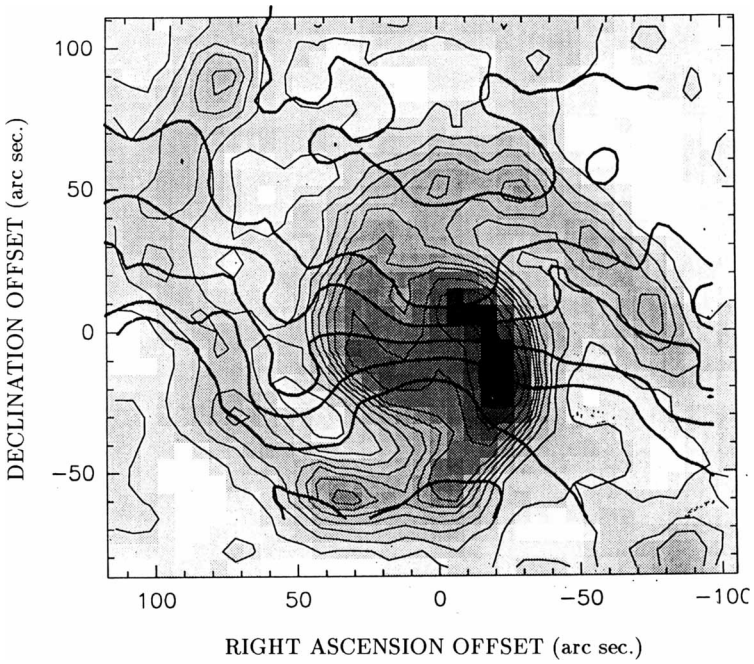

Figure 1. The ^{12}CO(2–1) integrated intensity contours (grey scale: lowest 5 K.kms^{-1}, highest 40 K.kms^{-1}) superposed on the first moment iso-velocity contours (from 400 kms^{-1} to the north to 520 kms^{-1} to the south by steps of 20 kms^{-1}). The central position is $\alpha(1950.0) = 13^h27^m46.1^s; \delta(1950.0) = 47 \circ 27'14''$

map shows a narrow ridge of CO emission, consisting of a chain of bright patches located along the dust lanes which run on the inner side of the spiral arms. These patches, in our map, fall right atop the highest (2–1) contours. The poor sensitivity of the interferometer to low spatial frequencies makes it miss the broad on-arm component (FWHP $\simeq 20''$ and about half of the CO (2–1) flux of the arms), and most of the interarm gas. The broad on-arm component of Fig. 1 covers the dust lanes as well as most of the HII regions.

Four radial bridges, connecting the two grand-design arms, are visible on Fig. 1. These bridges stand out more clearly on the peak intensity maps and seem associated with non-circular motions. They could correspond to an harmonic of the first density wave mode.

Fig. 2 shows the (2–1) line integrated intensity in a ring 0.5 kpc wide, 2 kpc in radius, as a function of azimuth. The ring is located in the plane of the galaxy, assuming a PA of -10° and an inclination of 20°. Intensities range from $\simeq$3 to 30 K.kms^{-1}, the smallest value being 3 times the r.m.s. noise. The arm and interarm components are fully resolved at this distance from the center and the intensity contrast is high. The contrast, defined as Imax/Imin, the ratio of the highest to the lowest intensities, reaches 10 for the southeast arm (azm= +60°). It is 6 if it is more conservatively defined as $\langle$Imax$\rangle$/$\langle$Imin$\rangle$, the ratio

https://doi.org/10.1017/S0074180900243556 Published online by Cambridge University Press

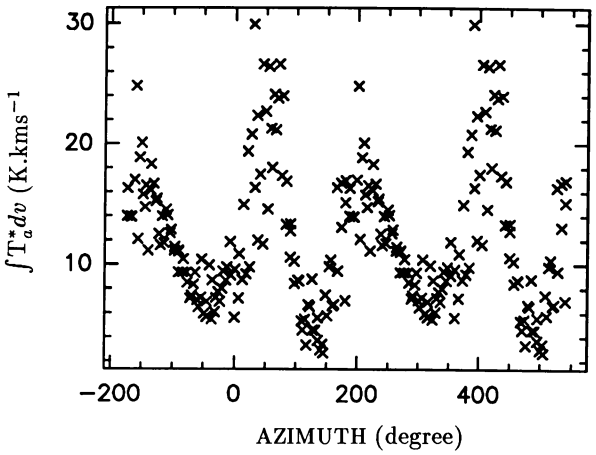

Figure 2. 4π azimutal distribution of the ^{12}CO(2–1) line integrated intensity at 2 kpc from the centre

of the arm crest average to the interarm dip average. As can be seen from Fig. 2, the contrast is smaller for the northeast arm (azm= −150°), so that the mean contrast for the 2 kpc ring is C=⟨Imax⟩/⟨Imin⟩=4.5 . Considering rings of different radii, we find that C remains roughly constant between 1.5 kpc and 6.5 kpc.

Comparing adjacent arm and interarm regions, rather than regions located at equal galactocentric radii, the arm-interam contrast can reach very large values locally: moving across the southern arm at declination –24″ to the adjacent interarm region, only 18″ away, where the nuclear disk component is much weaker, the (2–1) line integrated intensity drops by a factor of 17.

The strong non-circular motions, reported by Vogel et al. (1988) for the inner north-east arm (see also Rydbeck et al. 1985), are visible on both arms on Fig. 1, where they appear as distortions of the iso-velocity contours. The distortions in the arms are mirror-imaged by opposite distortions in the interarm region. Assuming the spiral arms are trailing, the non-circular motions behave as predicted by the density wave theory, i.e. the gas streaming inwards along the spiral potential well, then moving outwards and decelarating in the interarm region. Following this scenario, the line-of-sight components of the radial and tangential motions add in the NW and SE quadrants and substract in the NE and SW quadrants.

The large magnitude of the non-circular motions in and between the arms is visible on Fig. 3, which is a velocity-position diagram near the minor axis. These motions translate into a zig-zag pattern where different velocity components are nearly spatially coincident. As a part of this pattern we note an enhancement of the velocity dispersion in the arms.

The differences in velocity dispersion between the arm and interarm gas, as well as along the arms, are illustrated by the three profiles of Fig. 4: the left profile, observed toward a bright clump of the inner southwest arm, has a FWHP of 60 kms^{-1}; the middle profile,

https://doi.org/10.1017/S0074180900243556 Published online by Cambridge University Press

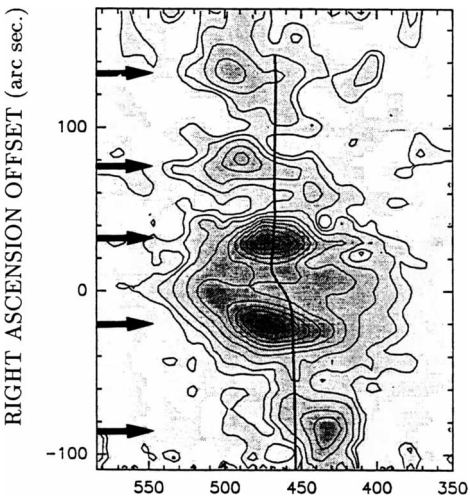

Figure 3. Strip at $-6''$ declination near the minor axis. Note the presence of strong deviations from circulation motion for the gas in the arm and in the interarm regions. The thick solid line represents pure circular motion and the arrows the position of the arms

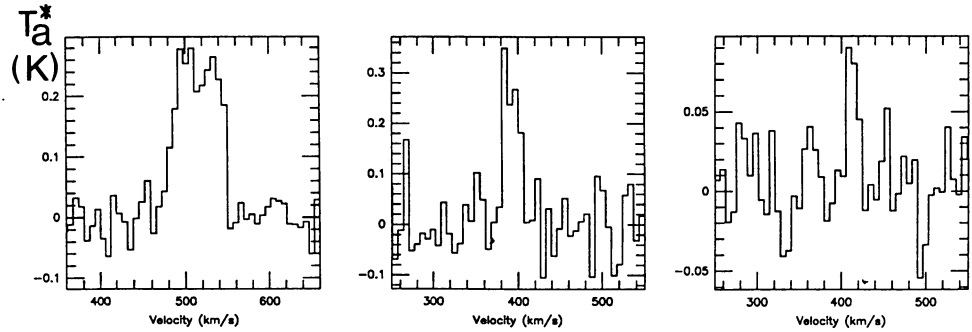

Figure 4. Three ^{12}CO(2–1) spectra, taken respectively at offsets $(36'', -54'')$ from the centre, in the inner region of the SE arm, (-72,54), further out in the same arm, and (48, 126) in the interarm region.

taken further out on the same arm, presumably near the co-rotation radius, has a FWHP of 20 kms^{-1}; the right profile, typical of the low intensity interarm component, a FWHP of

https://doi.org/10.1017/S0074180900243556 Published online by Cambridge University Press

15 kms^{-1}. The width of the left profile is surprising since the gradient of galactic rotation within the beam is less than 15 kms^{-1}. In-plane streaming motions would have to be very large to explain a 60 kms^{-1} linewidth. Cloud to cloud velocity dispersion in and perpendicular to the galactic plane must probably also be invoked; its large value could be linked to the strength of the density wave in that region.

The conversion of the CO line intensities into molecular column densities *a priori* is not straightforward and depends on the degree of excitation of CO, on the line optical depths, etc... Although it can be argued that the average $I(CO)/N(H_2)$ ratio in normal external galaxies may be similar to its average Milky Way value (see e.g. Young 1990), in which case the lowest solid contour of Fig. 1 corresponds to an H_2 column density $N(H_2)$ of $\simeq 4 \cdot 10^{21}$ cm^{-2} (or to a surface gas density σ of 80 $M_{\odot} pc^{-2}$) , $I(CO)/N(H_2)$ most probably varies between the arms and the interarm region. Only a multi-transition analysis of several molecular gas tracers can answer by how much. Table 1 shows some ratios involving the (2–1) and (1–0) lines of ^{12}CO and ^{13}CO. They argue for a multi-component model in which dense clouds, similar to the galactic giant molecular clouds, are embedded in a diffuse halo of low density gas (Garcia-Burillo et al. 1990).

TABLE 1: Average ratios of velocity-integrated brightness temperatures

	Central Disk	Inner arms	Interarm region
$^{12}CO(2\text{-}1)/^{12}CO(1\text{-}0)$	0.8	0.7	0.7
$^{12}CO(2\text{-}1)/^{13}CO(2\text{-}1)$	6	8	≥ 12
$^{12}CO(1\text{-}0)/^{13}CO(1\text{-}0)$	6	9	–

ACKNOWLEDGEMENTS

S.G.B thanks the CICYT(project PB88-0453) and ERASMUS network for their financial support during part of this work.

REFERENCES

Garcia-Burillo, S., Guélin, M., Despois, D. and Cernicharo, J. (1990) *in preparation*

Rand, R.J., and Kulkarni, S.R.(1989) *Ap.J.*,in press

Rydbeck, G.,Hjalmarson, A., and Rydbeck, O.E.H. (1985) *Astron. Ap.* **144**, 282

Tully, R.B. (1974) *Ap.J.* **27** ,449

van der Hulst,J.M.,Kennicutt,R.C.,Crane, P.C., Rots,A.H. (1988) *Astron. Ap.* **195**, 38

Vogel, S.N., Kulkarni, S.R., and Scoville, N.Z. (1988) *Nature* **334**, 402

Young, J.S. (1990) *The Interstellar medium in Galaxies* , p.67, H.A.Thronson and J.M. Shull (eds.), Kluwer Pub.

https://doi.org/10.1017/S0074180900243556 Published online by Cambridge University Press

Applause: Fran Verter, A. Poglitsch, A. Krabbe, Santiago Garcia-Burillo, Pierre Martin and Pierre Cox. In the background, Simon White, Josh Barnes.

https://doi.org/10.1017/S0074180900243556 Published online by Cambridge University Press